

See discussions, stats, and author profiles for this publication at: <https://www.researchgate.net/publication/257691186>

# Analysis of Bulk and Hydration Water During Thermal Lysozyme Denaturation Using Raman Scattering

ARTICLE *in* FOOD BIOPHYSICS · SEPTEMBER 2013

Impact Factor: 1.63 · DOI: 10.1007/s11483-013-9294-3

CITATIONS

5

READS

45

6 AUTHORS, INCLUDING:



**Giuseppe Bellavia**

Groupe ISA

6 PUBLICATIONS 70 CITATIONS

SEE PROFILE



**Yannick Guinet**

Université des Sciences et Technologies de ...

86 PUBLICATIONS 1,175 CITATIONS

SEE PROFILE



**Alain Hédoux**

Université des Sciences et Technologies de ...

94 PUBLICATIONS 1,240 CITATIONS

SEE PROFILE

# Analysis of Bulk and Hydration Water During Thermal Lysozyme Denaturation Using Raman Scattering

Giuseppe Bellavia · Laurent Paccou · Samira Achir ·  
Yannick Guinet · Jürgen Siepmann · Alain Hédoux

Received: 24 December 2012 / Accepted: 1 May 2013 / Published online: 19 May 2013  
© Springer Science+Business Media New York 2013

**Abstract** We describe a method for analyzing protein hydration by Raman spectroscopy on the model protein lysozyme. The analysis of the protein hydration shell is made possible by dissolving the protein in D<sub>2</sub>O, providing via isotopic exchange the uncoupled O–H stretching spectrum of water molecules early bound to the protein, which are thereafter spread into the solvent. The spectrum of the hydration water can be obtained by subtracting the spectrum of the contribution of D<sub>2</sub>O from that of the aqueous lysozyme solution in the intramolecular O–D stretching vibrations region (2,200–2,800 cm<sup>-1</sup>). Raman investigations were simultaneously carried out in the amide I region (1,500–1,800 cm<sup>-1</sup>) and in the O–D/H stretching spectrum (3,200–3,800 cm<sup>-1</sup>) during thermal denaturation of lysozyme, to analyze structural changes of the protein in relation to the physical properties of hydration water. It was found that the H-bond network of hydration water is slightly distorted compared to the bulk water at room temperature, with a loss of the tetrahedral local order. The difference between hydration and bulk water is significantly enhanced at T=90 °C in the denaturated state of the protein. The quantification of water molecules in direct interaction with the protein provides the temperature dependence of the solvent-accessible surface area during the denaturation process. Both kinds of information on hydration water and protein structure lead to a detailed description and overall understanding of the mechanism of protein denaturation.

**Keywords** Raman spectroscopy · Hydration water · Uncoupled OH stretch · Dilute DHO solution · Thermal denaturation · Lysozyme

## Introduction

It is recognized for more than 50 years that water has a fundamental role in protein stability [1]. More recently it was shown that a monolayer of water molecules was required for maintaining the protein functionality [2], suggesting the crucial role of the first hydration shell on protein folding, the protein structure and the conformational stability, the latter being a main issue in the field of pharmaceuticals as well as food and nutrition, which can allow better understanding and improving the mechanism at the basis of the food quality. Hence, deciphering the molecular mechanisms responsible for the stability of the tertiary and quaternary structures has led to analyze more specifically the structure and dynamics of hydration water surrounding the protein surface from experimental [3–8] or theoretical [4, 9–11] investigations, providing various descriptions of the water structure. Indeed, the structural organization of water in the hydration shell was described as more or less dense than in the bulk, or even as consisting of domains of different densities depending on whether they are located around hydrophobic or polar groups [12]. All experimental investigations carried out on the hydration dynamics reveals that water molecules around the protein surface have slower dynamics than in bulk [3, 13], showing that hydration water has a significant influence on the protein dynamics. However, different relaxation times are found depending on the experimental technique used (quasi-elastic neutron scattering [3, 14], NMR spectroscopy [5], or fluorescent probes [15]). Most of these investigations to analyze the properties of the interfacial water were performed at room temperature, while the analysis of the

G. Bellavia (✉) · L. Paccou · S. Achir · Y. Guinet · A. Hédoux  
Unité Matériaux Et Transformations, UMR CNRS 8207,  
Université Lille Nord de France, USTL,  
59655 Villeneuve d'Ascq, France  
e-mail: giuseppe.bellavia@univ-lille1.fr

J. Siepmann  
College of Pharmacy, INSERM U 1008, University of Lille, 3 Rue  
du Prof. Laguesse,  
59006 Lille, France

hydration shell during a process of denaturation could provide detailed insights on the parameters intimately related to the protein stability. On the other hand it is recognized that the solvent-accessible surface area (SASA) is directly connected to the protein stability and that the increase of the SASA is a signature of the protein unfolding, since the strong increase of conformational entropy which favours the unfolded state at high temperatures promotes the exposure of residues from the core of proteins to the solvent [16, 17].

Raman spectroscopy has been recognized as very useful to obtaining quantitative estimates of secondary structure, via the analysis of amide I band [18]. This band arises mainly from the C=O stretching vibration with minor contributions of the C–N stretching vibration and the N–H in-plane bend [18, 19]. The latter is responsible for the sensitivity of amide I band to N–H/N–D isotopic exchanges in the protein backbone. Several Raman investigations, carried out on different kinds of proteins dissolved in D<sub>2</sub>O, have shown that the amide I region is very suitable for monitoring the different stages of denaturation [20–25]. Actually, the modification of the tertiary structure is detected via enhanced isotopic H/D exchanges between proteins and interfacial water induced by the solvent penetration in the protein interior. However, no information has yet been obtained on the properties of hydration water from Raman spectroscopy for several reasons. First, Raman bands corresponding to the collective motions of water molecules are observed in the 30–200 cm<sup>-1</sup> range, overlapping with the internal and collective motions of the protein [22–24, 26]. Only indirect evidence of hydration water can be provided by comparing low-frequency spectra of proteins dissolved in water in presence and in absence of denaturants (urea or hydrochloride guanidine) [27]. Second, at physiological water concentrations, Raman spectra are dominated by the contribution of bulk water. Nevertheless, the use of D<sub>2</sub>O as solvent gives the opportunity to probe selectively OH groups within water molecules (DHO) resulting from isotopic exchanges between the H atoms of the protein surface and the solvent (D<sub>2</sub>O) around the protein surface which constitutes the water hydration shell. These water molecules diffuse into the solvent, though they give an estimation of the water molecules which were in direct interaction with the protein, i.e. located in the first hydration shell; they give a contribution to the spectrum of the intramolecular O–H stretching vibrations in the 3,000–3,600 cm<sup>-1</sup> region, while O–D stretching bands in the bulk solvent (D<sub>2</sub>O) are observed between 2,000 and 2,800 cm<sup>-1</sup>. Once the bulk contribution is subtracted, the spectral difference between the protein solution and the bulk solvent in the intramolecular O–D stretching region can give direct information on the hydration shell, in particular on the tetrahedral water network [28]. The intramolecular O–H stretching vibrations are very sensitive to the local H-bonding structure [21,

28–31], and could provide new information both on the interfacial water structure and on the protein surface as well as on the SASA, by estimating the number of water molecules.

In the present paper, we report the analysis of the solvent, originated by the H/D isotopic exchange on the surface of the model protein lysozyme dissolved in D<sub>2</sub>O, from Raman investigations in the intramolecular O–H, O–D stretching regions. Raman spectra in the amide I region were also taken to monitoring the thermal denaturation process, in order to analyze the alterations in the secondary structure of lysozyme in relation with the physical properties of hydration water.

## Experimental Methods

Lysozyme and D<sub>2</sub>O were purchased from Sigma. Lyophilized powder lysozyme has a purity minimum of 90 %, and isotopic purity for D<sub>2</sub>O is 99.990 atom % D. Lysozyme solutions were prepared by dissolving lysozyme in D<sub>2</sub>O (10 wt %) under nitrogen to prevent isotopic exchanges with the moisture of the ambient air. The solution was agitated in an Eppendorf agitator at room temperature (23 °C) during 2 h to ensure complete isotopic exchanges. Raman investigations were carried out on protein solutions at pH=6.5.

Non-polarized Raman spectra were measured with a Renishaw InVia Raman microspectrometer, comprising a single-grating spectrograph coupled to an optical Leica microscope. The 514.5 nm line of a Coherent Argon laser for excitation was used. Focusing the laser beam via a ×50 objective long-working distance objective leads to analyze a volume of about 25 μm<sup>3</sup>. The spectra were recorded in back scattering geometry in 4 min, with a resolution of 2 cm<sup>-1</sup> in the 1,500–3,800 cm<sup>-1</sup> frequency range, upon heating from 23 °C up to 90 °C using a THMS 600 Linkam temperature device. The lysozyme aqueous solution and the solvent were loaded in a cylindrical suprasil cell hermitically sealed to prevent the evaporation of water during heating the lysozyme solution.

## Results and Discussion

The high-frequency spectrum of lysozyme dissolved in D<sub>2</sub>O (LW<sub>d</sub>) was systematically taken between 1,500 and 3,800 cm<sup>-1</sup>. It was decomposed in two parts to be analyzed, (i) the amide I region between 1,500 and 1,800 cm<sup>-1</sup>, and (ii) the 2,000–3,800 cm<sup>-1</sup> spectrum dominated by the intramolecular O–D stretching bands, plotted in Fig. 1 at room temperature (23 °C). The solution was kept at 23 °C during more than 12 h. No significant change in the spectrum was

detected, indicating full H/D-exchange at room temperature in the native state of the protein. The spectrum of  $LW_d$  can be divided in 3 regions corresponding to the intramolecular stretching vibrations of the following bonds: (1) O – D ( $\nu_{OD}$ , 2,000–2,800  $\text{cm}^{-1}$ ) in bulk  $D_2O$ , (2) C – H ( $\nu_{CH}$ , 2,800–3,100  $\text{cm}^{-1}$ ) in lysozyme, and (3) O – H in DHO molecules ( $\nu_{OH}$ , 3,100–3,800  $\text{cm}^{-1}$ ) resulting from isotopic exchange between D atoms of the solvent and H atoms of lysozyme surface. The spectrum of the solvent ( $D_2O$ ) was also measured in 2,000–3,800  $\text{cm}^{-1}$  range. The contribution of O – H stretching bands to the spectrum of  $D_2O$  in region (3) is undetectable, indicating no significant H/D exchange between  $D_2O$  and the air during loading the solution in the cell. The intensity ratio between O – H and O – D stretching bands in the ( $LW_d$ ) spectrum is measured to be very close to 0.03. According to this, we have chosen to keep the same ratio for the DHO solution with no protein, used as a reference to untangle the effect of the protein from the solvent, by dissolving  $H_2O$  (3 wt %) in  $D_2O$ . The Raman spectrum in the 2,000–3,800  $\text{cm}^{-1}$  range of this DHO solution is compared in Fig. 1 to that of the protein solution. The  $LW_d$  spectrum is compared to those of DHO and  $H_2O$  in region (3) in the inset of Fig. 1.

The inset of Fig. 1 shows that the  $\nu_{OH}$  spectrum in DHO is significantly different from that in  $H_2O$ , in agreement with previous studies [31–33]. It can be observed in Fig. 1 that a dilute solution DHO in  $D_2O$  leads to a much narrower ( $\sim 500 \text{ cm}^{-1}$ ) OH stretching region (3) than that ( $\sim 700 \text{ cm}^{-1}$ ) in the spectrum of pure  $H_2O$ . The DHO spectrum is considered to be free of intermolecular coupling vibrations, and is called uncoupled stretching region. As a consequence, the shape of the DHO spectrum in region (3) is much simpler than that of  $H_2O$  and may be interpreted in terms of the local environment of the

water molecule. The DHO spectrum in region (3) clearly consists of two bands. The high-frequency band located around 3,600  $\text{cm}^{-1}$ , also observed in the ( $LW_d$ ) and  $H_2O$  spectra, is assigned to stretching vibrations in free OH groups [21, 30]. The low-frequency band in the spectrum of the uncoupled O – H stretching bands is observed around 3,440  $\text{cm}^{-1}$ , which is interpreted as reflecting quite strong H-bonding [32]. The width of this band, i.e. the breadth of the uncoupled O – H stretching bands in dilute DHO is observed to be much less than that in the  $H_2O$  spectrum for the coupled O – H stretching bands. However, uncoupled bands are very much broader than would be found in a non-H-bonded liquid [32]. These considerations on the frequency and width of uncoupled O – H stretching bands suggest that water molecules in dilute solution of DHO are involved in moderately strong H-bonding. The ( $LW_d$ ) spectrum in region (3) looks like that of the dilute DHO solution, except the observation of well defined shoulder in the low-frequency side of the uncoupled O – H stretching bands at room temperature (see inset of Fig. 1). This shoulder could be attributed either to N – H stretching vibrations of the protein backbone or to the O – H stretching vibrations in the protein structure.

The intramolecular O – D stretching spectrum of the bulk  $D_2O$  is plotted at 25 °C and at 90 °C in Fig. 2. It can be used to obtain structural information on the organization of water molecules [28]. The O – D and O – H stretching spectra can be analyzed in a similar way [33] and the fitting procedure requires three components [21, 29] localized by vertical dashed lines in Fig. 2. The low-frequency component ( $\nu_{OD1}$ ) around 2,380  $\text{cm}^{-1}$ , is usually considered as related to the tetrahedral organization of water molecules [28]. The component ( $\nu_{OD2}$ ) near 2,450  $\text{cm}^{-1}$ , corresponds to distorted tetrahedral arrangements, and the high-frequency band ( $\nu_{OD3}$ ) detected around 2,680  $\text{cm}^{-1}$  is assigned to free O – D groups corresponding to non-hydrogen bonded molecules. The spectrum of  $D_2O$  is superimposed to that of DHO in the 2,200–2,800  $\text{cm}^{-1}$  region (data not shown). It is consistent with the consideration that addition of a small amount of  $H_2O$  in  $D_2O$  does not change the local structure in  $D_2O$ , but only probes the structure. The spectrum of the hydration water can then be obtained by subtracting the spectrum of  $D_2O$  from that of the aqueous lysozyme solution. This spectrum is compared to that of bulk  $D_2O$  at 25 and 90 °C in Fig. 2. At 25 °C, the hydration water can be distinguished from the bulk by two main features shown by two arrows in Fig. 5: the intensity of the ( $\nu_{OD1}$ ) component decreases and the ( $\nu_{OD2}$ ) component slightly shifts toward the high frequencies. At 90 °C, these trends are observed to be significantly enhanced. The intensity decrease of the ( $\nu_{OD1}$ ) contribution reflects a loss of the tetrahedral organization in the hydration water, highly enhanced in the denatured state ( $T=90 \text{ }^\circ\text{C}$ ). The frequency upshift of the ( $\nu_{OD2}$ ) component indicates a decrease in the strength of

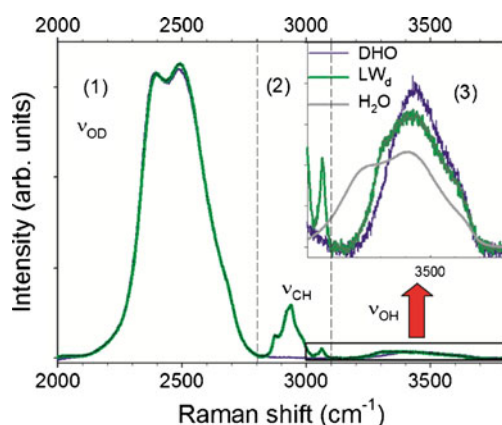


**Fig. 1** Raman spectra of lysozyme aqueous solution ( $LW_d$ ), DHO solution and  $H_2O$  in the 2,000–3,800  $\text{cm}^{-1}$  frequency range. The three spectral regions corresponding to O – D stretching bands (1), C – H stretching bands (2) and O – H stretching bands (3) are separated by vertical dashed lines. The inset shows a zoom of the framed area mainly corresponding to O – H stretching vibrations

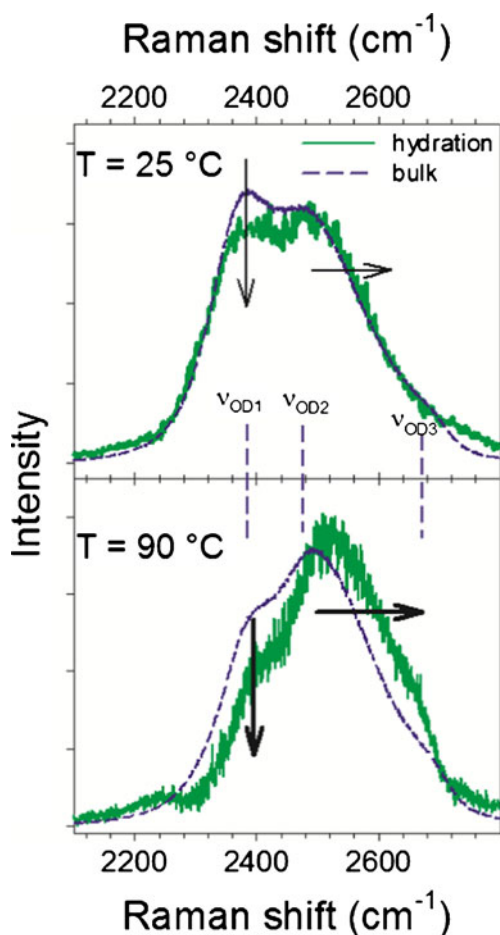


**Fig. 2** Raman spectra of intramolecular O – D stretching vibrations in bulk and hydration water at  $T=25$  and  $90$  °C

intermolecular D – O ... D bonding between  $D_2O$  molecules. The enhancement of the frequency shift at  $90$  °C indicates that water molecules are very disordered around denatured lysozyme compared to the organization in bulk  $D_2O$ .

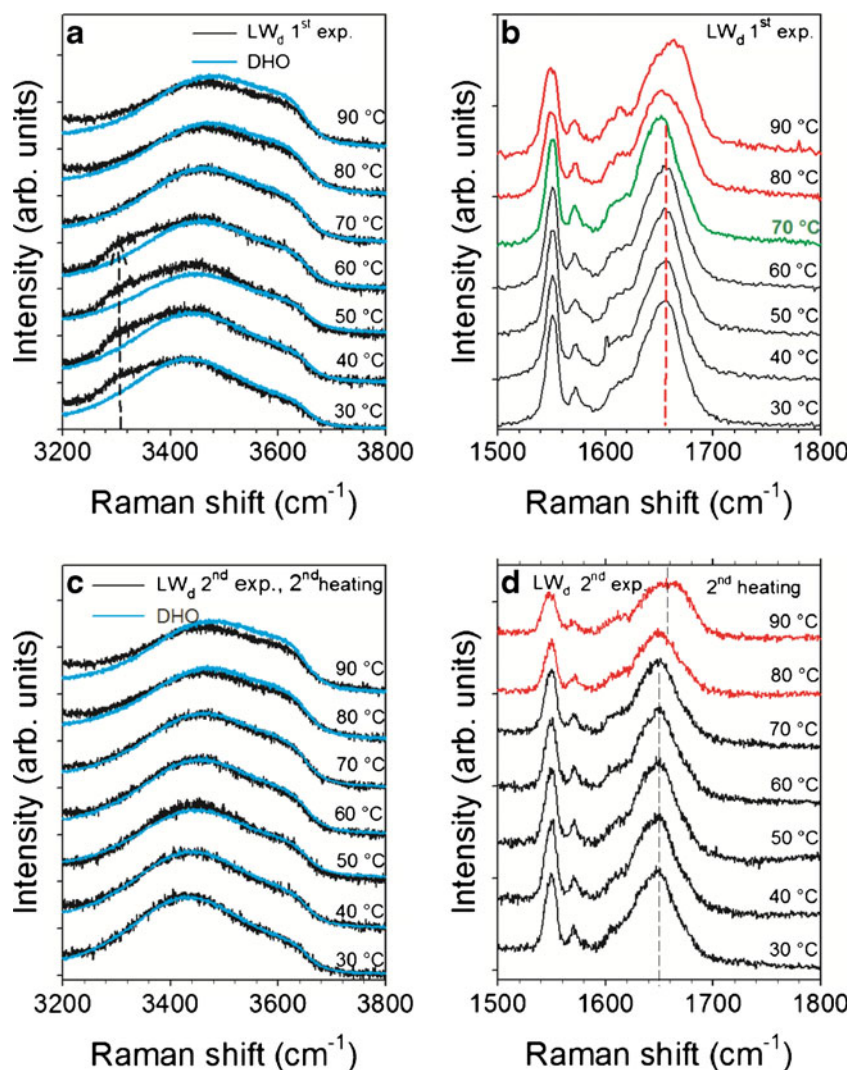
In order to distinguish among the effects due to the unfolding from those due to the isotopic exchange, two experiments were performed. In the first experiment, the lysozyme aqueous solution was heated from room temperature up to  $95$  °C. The temperature dependences of the ( $LW_d$ ) spectrum in region (3) and in the amide I region are plotted in Fig. 3a and b respectively. Figure 3a shows that upon heating, the additional band at  $3,310\text{ cm}^{-1}$ , attributed to the protein O – H stretching vibrations, is not detected from  $70$  °C up to  $90$  °C. Also, a clear frequency downshift of amide I band is evidenced in Fig. 3b at  $70$  °C. This frequency downshift of amide I band was interpreted as reflecting enhanced NH/ND isotopic exchange, associated with the penetration of the solvent in the protein interior [23, 34]. The contribution to the uncoupled O – H stretching spectrum disappears probably because of H/D exchange

between  $D_2O$  and buried OH/NH groups of the protein, which become exposed to the solvent upon heating around  $70$  °C. Above  $70$  °C, Fig. 3b shows that amide I band broadens and shifts toward the high frequencies, reflecting the unfolding process of the secondary structure [23], meanwhile Fig. 3a indicates that the O – H stretching spectrum of the lysozyme solution is congruent to that of DHO mixture, except for a slight frequency shift at the higher recorded temperatures.

In the second experiment, the protein solution was firstly heated up to  $70$  °C (1<sup>st</sup> heating), maintained at this temperature during 1 h, and cooled down to room temperature. The protein solution was then re-heated (2<sup>nd</sup> heating) from room temperature up to  $95$  °C. The temperature dependences of the ( $LW_d$ ) spectrum in region (3) and in amide I region are plotted for the 2<sup>nd</sup> heating in Fig. 3c and d respectively. Figure 3d shows that amide I band is localized around  $1,648\text{ cm}^{-1}$  at room temperature, i.e. the frequency of amide I mode after direct heating at  $70$  °C. No additional frequency downshift of amide I band is observed upon re-heating up to  $70$  °C, i.e. no enhanced NH/ND isotopic exchanges are detected. Only a frequency upshift is observed above  $70$  °C, usually interpreted as corresponding to the unfolding process of  $\alpha$ -helix structures [20, 23]. Figure 3c shows that, after cooling from  $70$  °C down to room temperature, the low-frequency contribution ( $\sim 3,310\text{ cm}^{-1}$ ) of OH groups of lysozyme to the O – H stretching spectrum is not detected. The spectra in the  $LW_d$  and DHO solutions can be superimposed with any noteworthy differences up to  $70$  °C. Above  $70$  °C, i.e. upon the unfolding process related to the secondary structure, a slight frequency shift between the two spectra is clearly detected, as observed in the first experiment (Fig. 3a). The amide I region were analyzed with the fitting procedure described in Fig. 4. Each band shape was fitted to the sum of a Lorentzian and a Gaussian function. The temperature dependences of the frequency of amide I band are plotted in Fig. 5a for both the first experiment and the second heating run of the second experiment. In the first experiment, Fig. 5a shows a downshift followed by an upshift of the Amide I band peak by increasing the temperature. The upshift represents the unfolding of the secondary structure, detected through its broadening and its frequency upshift. The downshift can not be evidenced in presence of normal water but only in heavy water: it is related to the H/D exchange when the exposure to the solvent of the inner sites of the protein occurs. Several models have been proposed to explain the downshift, either as a global unfolding with a kinetic mechanism [25] or as reflecting the penetration of  $D_2O$  within the protein. At this stage, the protein was considered in a pre-denatured state [23, 24], the so-called “molten globule” state [35–38], described as a water-swollen tertiary structure, highly flexible, with intact secondary structure.



**Fig. 3** Temperature dependence of the Raman spectrum of lysozyme aqueous solution ( $LW_d$ ): - in the 1<sup>st</sup> experiment, **a** in the OH stretching region (3) between 3,200 and 3,800  $\text{cm}^{-1}$  and **b** in the amide I region between 1,500 and 1,800  $\text{cm}^{-1}$ ; - in 2<sup>nd</sup> heating of the 2<sup>nd</sup> experiment, **c** in region (3) and **d** amide I region. The  $LW_d$  spectra in region (3) are compared to that of DHO at each temperature



In the second experiment, only the unfolding process can be detected, since the equilibrium of NH/ND isotopic exchanges between  $D_2O$  and H atoms of lysozyme reached at 70 °C is maintained upon cooling at room temperature. The same phenomenon, for H/D isotopic exchanges, explains why the Raman band located at 3,310  $\text{cm}^{-1}$ , is not observed at room temperature after cooling from 70 °C in the second experiment.

The analysis of the spectrum of DHO solution shows that the intensity ratio between OH and OD stretching bands give the weighted concentration of OH groups involved in water molecules (3 %) with an uncertainty of 5 %. If we adopt the consideration that isotopic exchanges between  $D_2O$  and NH, OH groups of lysozyme give rise to OH groups in water molecules which diffuse from the protein surface into the solvent, the intensity ratio between OH and OD stretching bands represents the proportion of water molecules bound to the protein with respect to the bulk. After subtracting the OH contribution of the protein to the OH stretching mode spectrum, the ratio  $\rho_{OH} = I_{OH}/I_{OD} =$

$0.0246 \pm 0.0015$  is obtained at room temperature, without thermal treatment of the protein solution. The number of water molecules ( $n_w$ ) bound to the lysozyme surface can be estimated by:

$$n_w = \frac{\rho_{OH} / (g_{LYS} / g_{D_2O})}{MW_{D_2O} / MW_{LYS}} \quad (1)$$

where  $MW_{D_2O}$  and  $MW_{LYS}$  are the molecular weights of  $D_2O$  and lysozyme respectively, and  $g_{LYS}/g_{D_2O}$  corresponds to the weight ratio of lysozyme in  $D_2O$ , equal to 1/9. Then  $\rho_{OH}$  value indicates that at room temperature a lysozyme molecule is surrounded by a bound layer of  $158 \pm 8$  water molecules in the native state of lysozyme. This value is found in very good agreement with recent dielectric spectroscopy investigations [8] leading to the determination of  $165 \pm 15$  water molecules bound to the lysozyme surface. Hence,  $\rho_{OH}$  can be considered as a parameter directly representative of the SASA. The ratio  $\rho_{OH}$  was measured upon the first and second heating runs of the second experiment

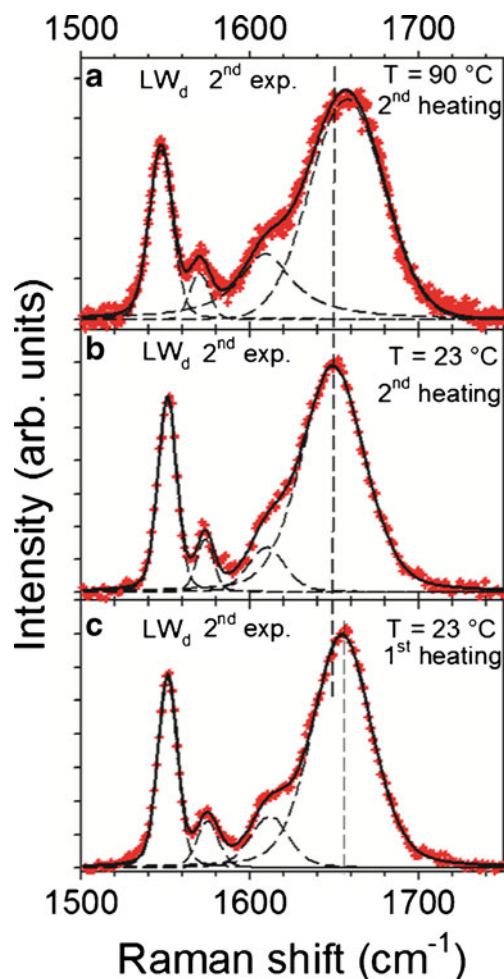


**Fig. 4** Fitting procedure of the Raman spectra in the uncoupled O – H stretching region (3): **a** At  $90^\circ\text{C}$ , in the 2<sup>nd</sup> heating of the 2<sup>nd</sup> experiment on  $\text{LW}_d$  solution; **b** At  $23^\circ\text{C}$ , in the 2<sup>nd</sup> heating of the 2<sup>nd</sup> experiment on  $\text{LW}_d$  solution; **c** At  $23^\circ\text{C}$ , in the 1<sup>st</sup> experiment on the  $\text{LW}_d$  solution. The solid lines correspond to fitting spectra, and dashed lines to the components used in the fitting procedure (sum of a Lorentzian and Gaussian function)

and reported in Fig. 5b, and the temperature dependence  $\rho_{\text{OH}}(T)$  was interpreted as reflecting the changes in the SASA. It is firstly observed that the proportion of OH groups increases between 60 and  $75^\circ\text{C}$ , as the frequency of amide I band decreases. At about  $73^\circ\text{C}$ , the number of water molecules bound to the protein in the molten globule state was estimated to  $212 \pm 11$ , indicating the increase of the SASA by a factor 1.3. Secondly, after cooling to room temperature from  $73^\circ\text{C}$ , the proportion of OH groups is almost identical to that determined at  $73^\circ\text{C}$  upon the first heating. Thirdly, upon the second heating, an additional increase of  $\rho_{\text{OH}}$  is observed above  $75^\circ\text{C}$ , i.e. when the protein denatures. The SASA is estimated 1.75 times greater in the denatured state. It is worth noting that the reported investigations on solvent–protein interactions, via the detection of H/D isotopic exchanges, show a clear correlation

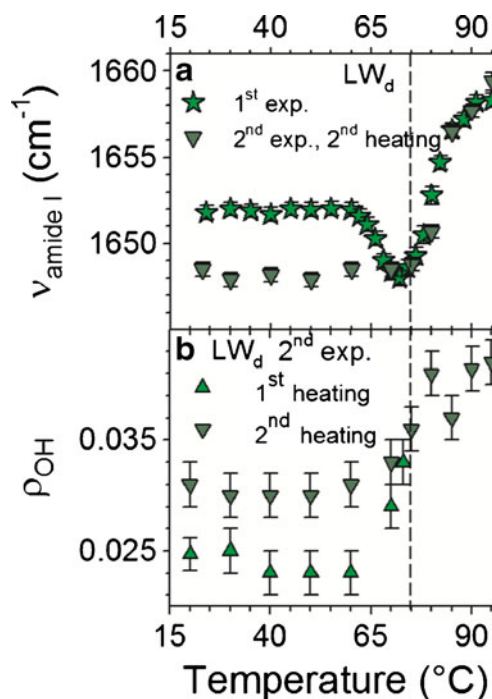


**Fig. 5** Data analysis resulting from fitting procedure of Raman spectra of the  $\text{LW}_d$  solution: **a** In the amide I region: temperature dependence of the frequency of amide I mode upon heating. Stars correspond to the first experiment, and triangles down to the 2<sup>nd</sup> heating of the 2<sup>nd</sup> experiment; **b** In region (3):  $\rho_{\text{OH}}$ , corresponding to the ratio between intensities of O – H and O – D stretching spectrum; triangles up and down respectively correspond to the first and second heating of the second experiment

between the results obtained from the analysis of amide I mode and that of the O – H and O – D stretching spectra.

## Conclusions

We report in the present study the first investigation by Raman spectroscopy of the water hydration of lysozyme. This analysis is made possible by dissolving the protein in  $\text{D}_2\text{O}$ , then evaluating selectively by isotopic exchanges the intramolecular O – D and O – H stretching spectra, which provide direct information on the protein-solvent interactions during the whole denaturation process. The former, representative of the hydration water, was compared to the bulk  $\text{D}_2\text{O}$ , whereas the latter was compared to that of a dilute DHO solution obtained by dissolving 3 % of  $\text{H}_2\text{O}$  in  $\text{D}_2\text{O}$ . The O – D spectrum comparison led to evidence a loss of the tetrahedral organization in the hydration water, in which the disorder of water molecules around the lysozyme is highly enhanced in the denatured state, compared to the organization in bulk  $\text{D}_2\text{O}$ . The analysis of the O – H spectrum allows the estimation of the number of water molecules constituting the first hydration layer, from the intensity ratio

$\rho_{\text{OH}}$  which can be considered as a parameter directly representative of the SASA.

This study shows that Raman investigations in the 1,500–3,800  $\text{cm}^{-1}$  frequency range on a protein dissolved in  $\text{D}_2\text{O}$  give a detailed analysis of the protein denaturation. Indeed, the successive modifications of the tertiary and secondary structures can be observed via the analysis of the amide I mode, with the associated changes of the SASA determined from the uncoupled O–H stretching spectrum. The physical properties of interfacial water (strength of H-bonding, SASA, water network structure), can bring out important information on the mechanism of protein denaturation by different sources of stress (temperatures, pressure, dehydration, denaturants, ...) but also on the mechanism of stabilization by bioprotectant agents.

**Acknowledgments** This work was supported by the ANR (Agence Nationale de la Recherche) through the BIOTAB project (“Physique Chimie du Vivant” program), by FEDER and Nord-Pas de Calais region.

## References

1. W. Kauzmann, Adv. Protein Chem. **14**, 1 (1959)
2. G. Careri, Collective Effects in Hydrated Proteins, in *Hydration Processes in Biology: Theoretical and Experimental Approaches*, ed. by M.-C. Bellissent-Funel (Ios Press, Amsterdam, 1999)
3. S. Dellerue, M.-C. Bellissent-Funel, Chem. Phys. **258**, 315 (2000)
4. M. Tarek, D.J. Tobias, Biophys. J. **79**, 3244 (2000)
5. K. Modig, E. Liepinsh, G. Otting, B.J. Halle, Am. Chem. Soc. **126**, 102 (2004)
6. C. Mattea, J. Qvist, B. Halle, Biophys. J. **95**, 2951 (2008)
7. D.I. Svergun, S. Richard, M.H.J. Koch, Z. Sayers, S. Kuprin, G. Zaccai, Proc. Natl. Acad. Sci. USA **95**, 2267 (1998)
8. N.Q. Vinh, S.J. Allen, K.W.J. Plaxco, Am. Chem. Soc. **133**, 8942 (2011)
9. C. Schroder, T. Rudas, S. Boresch, O.J. Steinhauser, Chem. Phys. **124**, 234907 (2006)
10. A. Oleinikova, N. Smolin, I. Brovchenko, Biophys. J. **93**, 2986 (2007)
11. A.R. Bizzari, S. Cannistraro, Phys. Rev. E **53**, R3040 (1996)
12. F.M. Richards, Ann. Rev. Biophys. Bioeng. **6**, 151 (1977)
13. C. Bon, A.J. Dianoux, M. Ferrand, M.S. Lehmann, Biophys. J. **83**, 1578 (2002)
14. M.-C.J. Bellissent-Funel, Mol. Liq. **84**, 39 (2000)
15. B. Bagchi, Chem. Rev. **105**, 3197 (2005)
16. S.N. Timasheff, PNAS **99**, 9721–9726 (2002)
17. T. Arakawa, S.N. Timasheff, Biochemistry **21**, 6536–6544 (1982)
18. R.W. Williams, A.K.J. Dunker, Mol. Biol. **152**, 783 (1981)
19. W.K. Surewicz, H.H. Mantsch, D. Chapman, Biochemistry **32**, 389 (1993)
20. R. Ionov, A. Hédoux, Y. Guinet, P. Bordat, A. Lerbret, F. Affouard, D. Prevost, M. Descamps, J. Non-Cryst. Solids. **2006**.
21. A. Hédoux, Y. Guinet, L.J. Paccou, Phys. Chem. B **115**, 6740 (2011)
22. A. Hedoux, J.F. Willart, L. Paccou, Y. Guinet, F. Affouard, A. Lerbret, M.J. Descamps, Phys. Chem. B **113**, 6119 (2009)
23. A. Hédoux, R. Ionov, J.F. Willart, A. Lerbret, F. Affouard, Y. Guinet, M. Descamps, D. Prevost, L. Paccou, F. Danède, J. Chem. Phys. **124**, 14703 (2006)
24. J.-A. Seo, A. Hedoux, Y. Guinet, L. Paccou, F. Affouard, A. Lerbret, M. Descamps, J. Phys. Chem. **B114**, 6675 (2010)
25. P. Sassi, G. Onori, A. Giugliarelli, M. Paolantoni, S. Cinelli, A.J. Morresi, Mol. Liq. **159**, 112 (2011)
26. L. Fu, S. Villette, S. Petoud, F. Fernandez-Alonzo, M.-L.J. Saboungi, Phys. Chem. B **115**, 1881 (2011)
27. A. Hédoux, S. Krenzlin, L. Paccou, Y. Guinet, M.P. Flament, J. Siepmann, Phys. Chem. Chem. Phys. **12**, 13189 (2010)
28. A. Lerbret, P. Bordat, F. Affouard, Y. Guinet, A. Hedoux, L. Paccou, D. Prevost, M. Descamps, Carbohydr. Res. **340**, 881 (2005)
29. G. D’Arrigo, G. Maisano, F. Mallamace, P. Migliardo, F.J. Wanderlingh, Chem. Phys. **75**, 4264 (1981)
30. G.E.J. Walrafen, Chem. Phys. **47**, 114 (1967)
31. J.R. Scherer, M.K. Go, S.J. Kint, Phys. Chem. **78**, 1304 (1974)
32. T.T. Wall, D.F.J. Hornig, Chem. Phys. **43**, 2079 (1965)
33. W.F. Murphy, H.J.J. Bernstein, Phys. Chem. **76**, 1147 (1972)
34. A. Hedoux, F. Affouard, M. Descamps, Y. Guinet, L. Paccou, Phys.: Condens. Matter **19** (2007). 8 p
35. K. Kuwajima, Proteins **6**, 87 (1989)
36. J. Baum, C.M. Dobson, P.A. Evans, C. Hanley, Biochemistry **28**, 7 (1989)
37. K. Masaki, R. Masuda, K. Takase, K. Kawano, K. Nitta, Protein Eng. **13**, 1 (2000)
38. P.L.J. Privalov, Mol. Biol. **258**, 707 (1996)